Proceedings World Geothermal Congress 2005
Antalya, Turkey, 24-29 April 2005

Numerical Modeling of the Momotombo Geothermal System, Nicaragua

Enrique A. Porras, Toshiaki Tanaka, Hikari Fujii and Ryuichi Itoi

Department of Earth Resources Engineering, Faculty of Engineering, Kyushu University, Fukuoka 812-8591, Japan

E-mail address, ep2107@mine.kyushu-u.ac.jp

Keywords: Geothermal, numerical modeling, hydrogeology.

ABSTRACT

The Momotombo geothermal field is located on the northwestern shore of Lake Managua and on the southwestern slope of the active Momotombo Volcano, Nicaragua. The field has been producing steam since 1983 and has an installed capacity of 77 MWe with 47 wells drilled in an area of 2 km^2. There are three permeable layers at Momotombo: a shallow layer can be found between 200 and 700 m b.s.l., the other two are located at 700 to 1500 m b.s.l., and 1500 to 2000 m b.s.l.. The hydrogeological model of the reservoir indicates that a major upflow related to NE-SW trending faults presents below the western part of the well field. The producing wells in the eastern half of the field are fed by shallow lateral flow from the major upflow. Temperature profiles of shallow wells in the eastern part support a presence of an inflow of low temperature fluid from the southeastern part of the well field and below the shallow reservoir of high temperature. Three-dimensional numerical model consisting of 1863 grid blocks was developed for reservoir simulations, and then natural state simulation of Momotombo, production and injection simulations for more than 20 years of exploitation were carried out with this model using AUTOUGH2 and iTOUGH2 simulators.

1. INTRODUCTION

The Momotombo geothermal field is situated on the northwestern shore of Lake Managua and at the foot of the active Momotombo volcano. The field has been developed by National Entities of Nicaragua (National Institute of Energy (INE) and Nicaraguan Electric Company (ENEL)), since the commissioning of the power plant in 1983 up to 1999, when ORMAT Momotombo Power Company continued with the development and exploitation of the field. To date, 47 wells have been drilled in an area of about 2 km^2 during the four drilling stages (1974 - 78, 1981 - 85, 1992 - 96 and 2000 - 02), varying in depths from a few hundred meters to as deep as 2,839 m. The drilling results have shown the presence of high temperature systems at three different depths: 200 - 400 m below sea level (m b.s.l.) with 200-230°C, 800 - 1700 m b.s.l. with 250 - 290°C, and a deep zone (>2000 m b.s.l) with temperature higher than 325°C. Two layers at the shallower zones have good permeability, but the deep one has relatively low permeability. The geothermal reservoir is of water-dominated type and the water is of sodium – chloride type (Verma, 1996). In this field, Bjornsson and Porras (2001) developed a conceptual reservoir model where high temperature fluids upflow in the southwestern area of the field through NE-SW faults, then flows laterally in the permeable zones at depths 800 – 1400 m b.s.l. and also flows to the south-east through NW-SE faults at depths 200 – 400 m b.s.l. Well outputs range between 1 – 8 MWe. Fig. 1 shows location of wells at Momotombo.

The primary objective of the present work is to develop a numerical model of the Momotombo geothermal field that can be used to predict the future behavior of production wells, the effects of reinjection, and the overall depletion of the geothermal reservoir. The model is three-dimensional and well-by-well, which allows for history matching of flow rate and enthalpy data from all wells and pressure draw down in the reservoir. The present model is capable to predict future mass production decline of the existing wells, generation capacity and effects of injection on well behaviors.

2. FIELD DEVELOPMENT

The field has been operating since 1983 with an installed capacity of 70 MWe with two units of 35 MWe condensing type. The second unit started electricity generation in September 1989, since then the output declined steadily down to 8 MWe by July 1999. The reservoir pressure dropped at a rate of 2 bars/year and, this induced an extensive boiling in the shallow reservoir. Consequently, quick intrusion of low temperature water into the reservoir occurred and then resulted in cooling of the shallow reservoir. At the same time, temperature declined at shallow wells, MT-5, 12, 17, 20 and 22, down to 170 – 180°C. As a result, these wells failed to discharge because of reservoir pressure decline and temperature drop as well.

A rehabilitation program to improve reservoir management as well as to sustain stable operation of the plant was started in June 1999 under the new administration (ORMAT Momotombo Power Company).

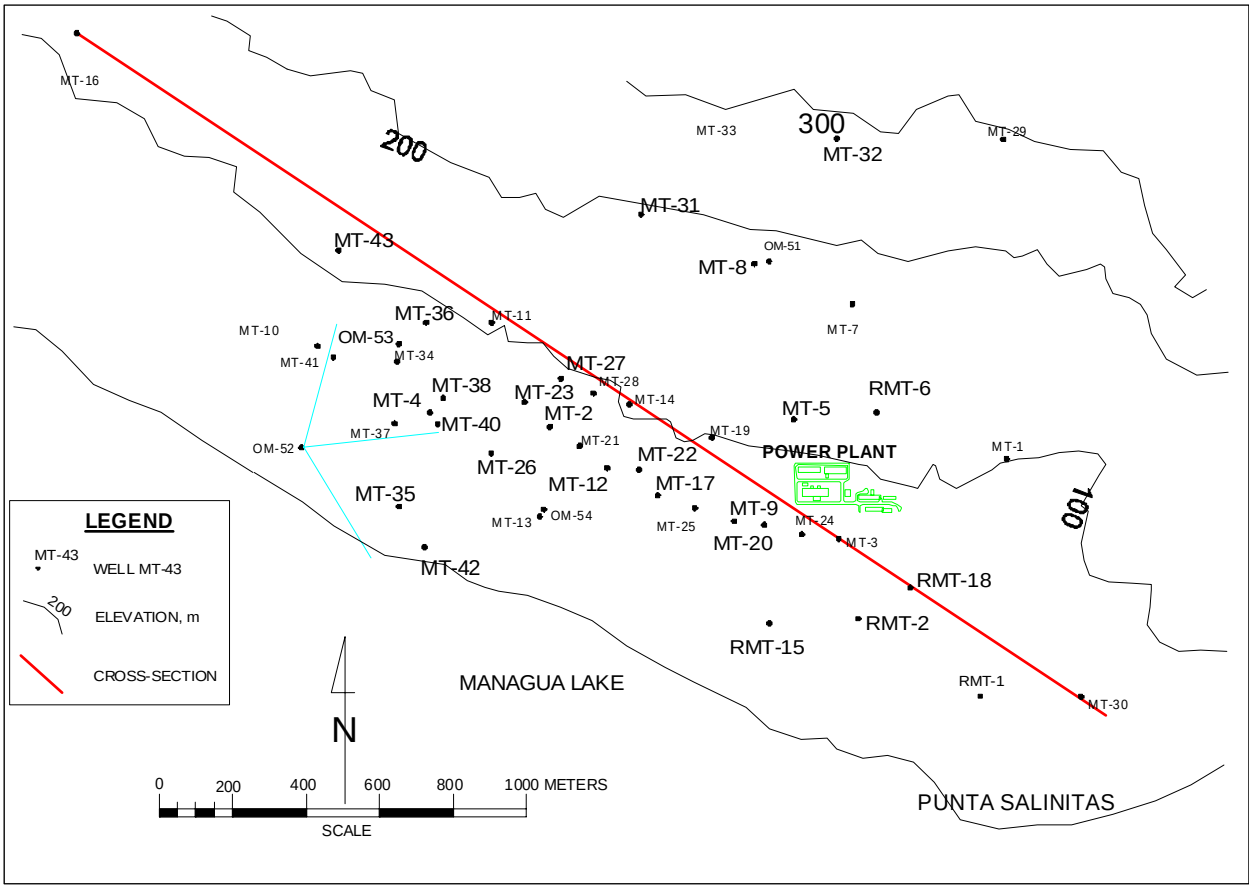

Figure 1: Wells location at Momotombo

This program consists of:

1) Work over for existing production wells. This includes cleaning calcite scale deposited in wellbore, mechanical repairing failures and cementing jobs. After the mechanical cleaning in wellbores succeeded, calcite inhibitor pumping was started into wells at MT-2, 4, 23, 26 and 27. Three production wells (MT-4, 35 and 42) were also treated with acid in order to clean calcite scale formed in formation near well bore. A second stage of acid job was carried out at the end of 2003, pumping acid into MT-42 and MT-35, with poor results.

2) Drilling four new deep wells (>2000 m). The new targets were selected in the western part of the field from a series of geophysical surveys. The only successful well was OM-53 that produced about 85 t/h of steam (more than 30 % of the total steam supplied to the power plant).

3) Reinjecting 100% of the separated water into the formation in order to moderate reservoir pressure decline.

4) Installing a new unit of combined cycle with capacity of 7 MWe by using separated water at 150°C.

5) Carry out three-dimensional simulation of the geothermal system, and the results provide information for a new exploitation strategy.

As a result of this power recovery program, the net power generation reached to 35 MWe.

3. GEOLOGICAL SETTING

Geologically the field is developed in the scope of the Nicaragua Depression filled up with volcanic and volcano-sedimentary pre-Quaternary materials (Fig. 2). The figure also shows the structural frame of the field, where it can be observed that the area is characterized mainly by three faults systems: NW-SE; NE-SW and N-S faults. The first two systems are correlated with the regional tectonics of the Nicaragua graben (“Puerto Sandino fault”, with NE-SW direction, and “Boundary fault of Puerto Momotombo Graben”, with NW-SE direction), whereas between N-S alignments, there are regional faults extending to the center of the Momotombo volcano. The set of these faults allows the circulation of the fluids in the field. In particular, the

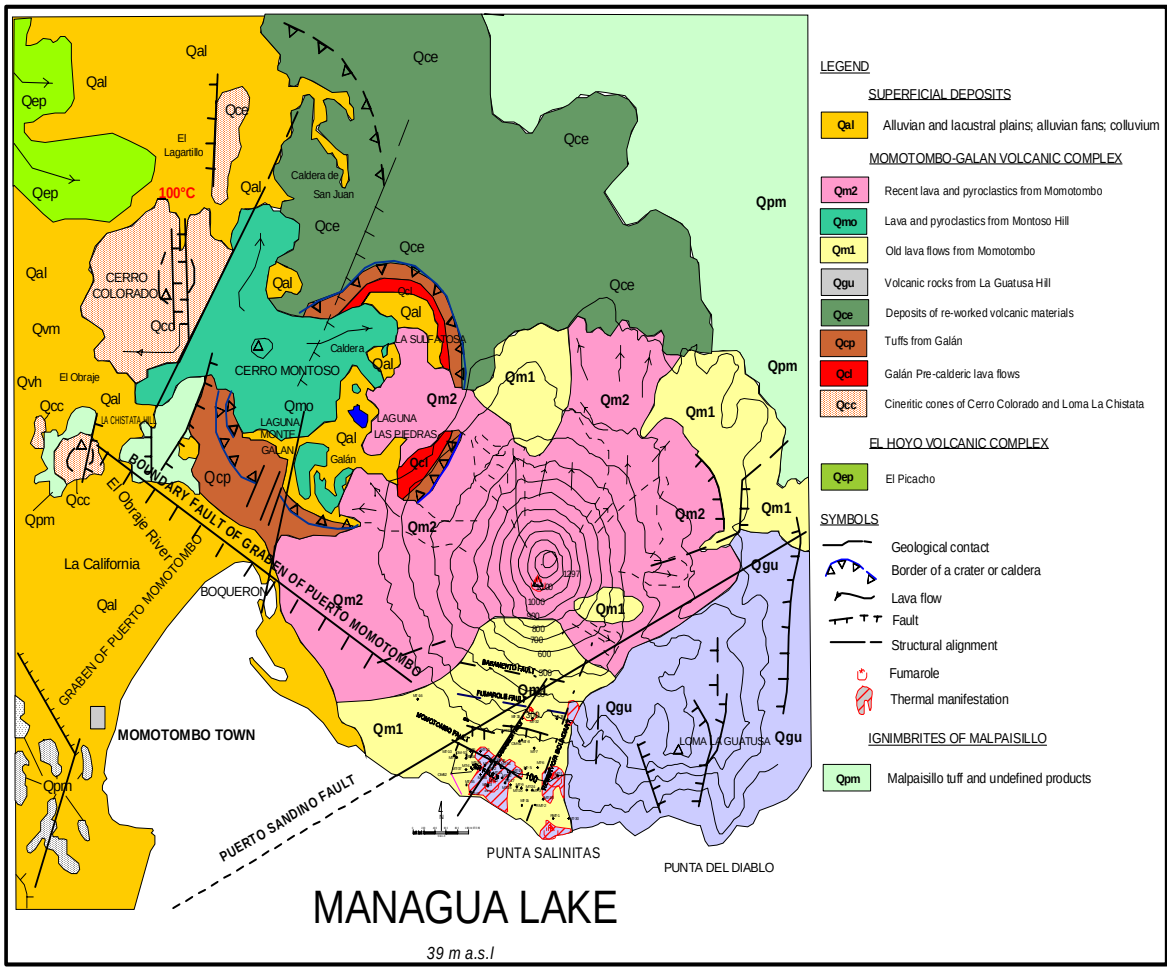

Figure 2: Geological map and structural frame of Momotombo area (after Geothermex, Inc., 2001)

recharge of the shallow reservoir occurs in coincidence with a fractured zone generated by the intersection of faults of these three systems, and the most productive wells are located generally in correspondence to structural crossings.

Based on the petrographic and macroscopic analysis of drilling cuttings and some cores, the lithology of Momotombo geothermal field has been divided into six lithological units that consist of andesite and andesite-basaltic volcanic products, volcano-clastic deposits, different kinds of tuffs, volcano-sedimentary and sedimentary deposits, and some sub-intrusive bodies and dikes. From the geological interpretation of these units, it can be seen a long period of volcanic activity in the area, that has generated around 1,700 m thickness of different volcanic and volcano-sedimentary products, and the presence in the deeper zones of sedimentary rocks combined with volcanic rocks. All these units had been formed from Early Miocene to Quaternary..

Unit I:

It belongs to Quaternary volcanism and it is located between 0 and 260 m b.s.l., consisting of andesite, andesite-basaltic lava flows, inter-layered with scoriae and some local epiclastic and lake sediments.

Unit II:

It is located between 260 m b.s.l. to 600-800 m b.s.l. This unit was formed by a basal-clastic and lavic portion and by an over layered tuff sequence of andesite-dacite composition. The upper part, formed by andesite-dacite vitro and crystal tuff deposits with ash matrix, followed by a volcano-clastic deposits and lava flows of Tertiary volcanism, that conform the lower part of the unit.

Unit III:

This unit can be seen at different depths, between 600-800 m b.s.l to 1500-1700 m b.s.l. and consists of mainly volcanic products in the east of the field, that changes gradually to a sedimentary deposits of continental origin to the west. It consists of clastic tuff and crystal tuff of heterogeneous composition, sandstone of red brown color, volcano-sedimentary deposits and volcanic products of andesite, andesite-basaltic and andesite-dacite composition.

Unit IV:

This unit consists of volcano-sedimentary layers, mostly of tuffaceous deposits of “ignimbrite type”, with very low presence of lava flows. The unit has been recognized from 1600-1700 m b.s.l. to 2000 m.b.s.l., with thickness of 400 to 500 m.

Unit V:

This is a sedimentary unit with thickness of 360 m and consists of intercalations of lutite/argillite with marl sediments. Abundant fossils (woods and seeds, some foraminifers are filled with pyrite) have been found in this unit (wells MT-43 and OM-52).

Unit VI:

The upper part of this unit is located at 2,355 m b.s.l., on the other hand, the depth of its bottom is unknown. It is a volcanic, volcano-clastic sequence consisting of green crystal and clastic tuffs, some andesite lava flows and a volcano-clastic sandstone.

4. GEOPHYSICAL SETTING

Geophysical explorations were carried out in Momotombo in seven different periods between 1970 and 2000. During 70's and early 80's the geophysical studies were carried out as part of the pre-feasibility for the development of the geothermal field. The most recent ones (DAL SpA, 1995 and TRANSPACIFIC, 2000) correspond to studies related with the steam production recovery, locating some of the main hydro-geological features of the Momotombo geothermal system.

In 2000, TRANSPACIFIC carried out four different surveys such as self-potential, gravimetry, aeromagnetic and micro-earthquake monitoring to locate main faults at depth in the field. Fig. 3 shows Bouguer gravity map. Iso gravity lines extend NNW to SSE where well field locate in the southern part. Thus, the results imply that northwestern part of the area may act as recharge zone, with a plateau like gravity values followed by descending gravity.

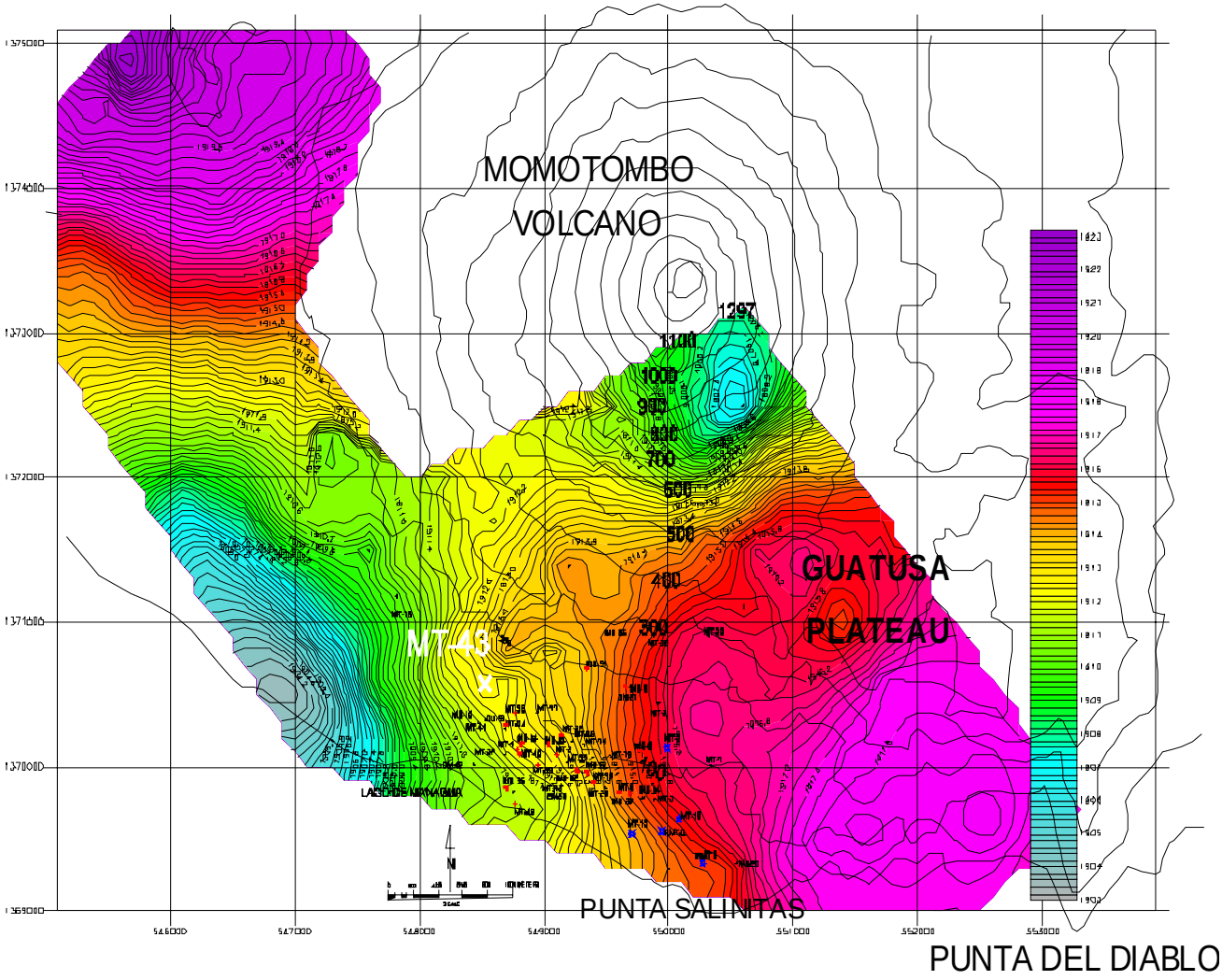

Figure 3: Simple Bouguer Gravity Map (After TRANSPACIFIC, 2000)

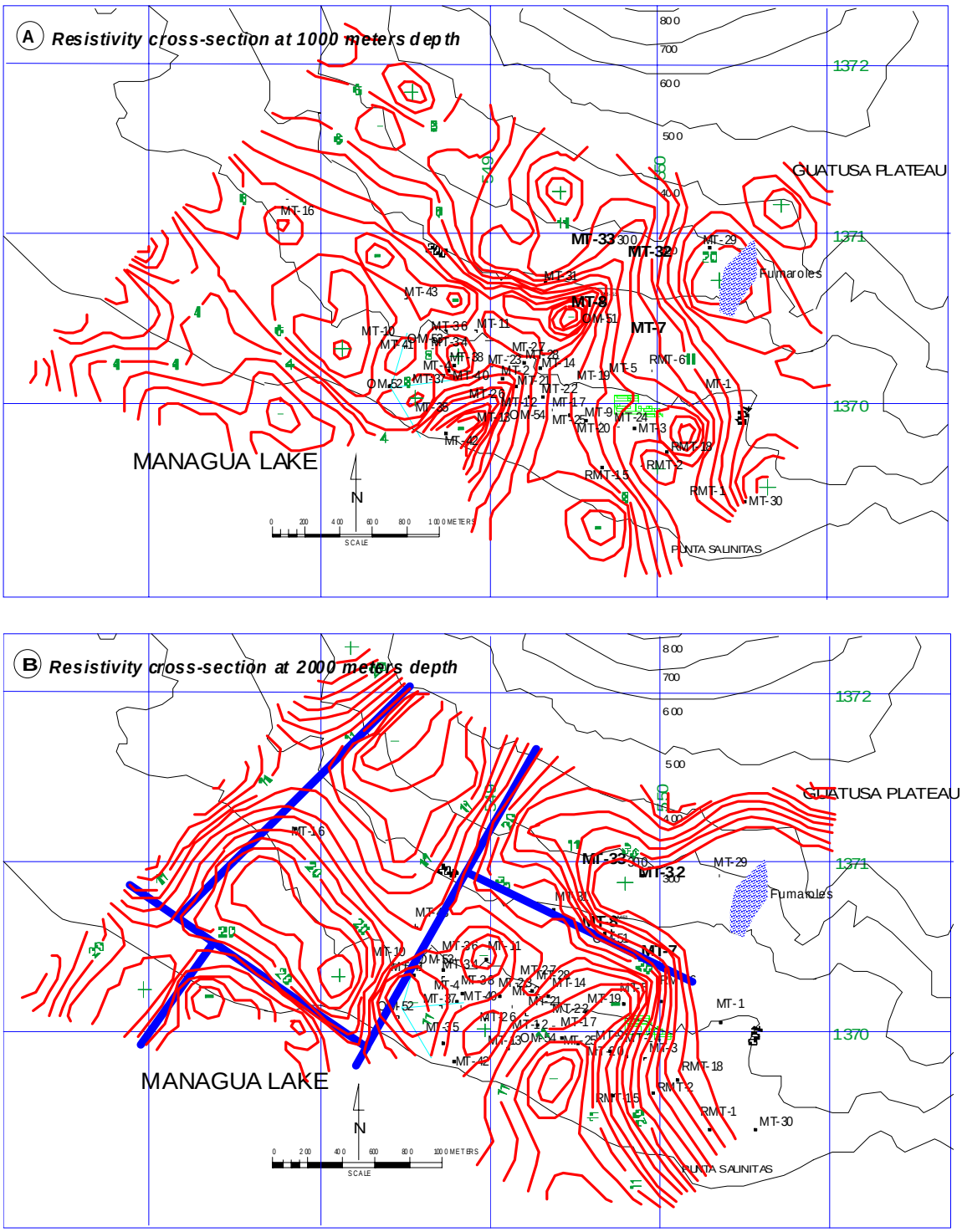

Figure 4: Resistivity contours at 1000 and 2000 m depth (after DAL SpA and TRANSPACIFIC)

Fig. 4 (A and B) shows the resistivity contours at 1000 and 2000 m depth carried out in 1995 by DAL SpA. TRANSPACIFIC analyzed the results of the survey, and their analysis coincided that the area of higher elevation compared with the wellfield is characterized by high resistivity where a large fumaroles present. A sharp WNW resistivity boundary separates the low-resistivity area of the main wellfield from the area where wells MT-7, MT-8, MT-32 and MT-33 locate (Fig. 4A), and this trend is also evident at 2000 m depth (Fig. 4B). This resistivity pattern at depth suggests presence of possible fractures along the various resistivity boundaries. An additional feature is that the most active fumaroles features indicated by blue dotted zone lies in the vicinity of the wellfield and also to the west of the Guatusa Plateau (Fig. 4A and B).

5. PREVIOUS MODELING STUDIES

The first numerical model of the Momotombo geothermal system was developed in 1983 by ELC-Electroconsult (Electroconsult, 1983) as part of the feasibility study of the second 35 MWe unit. The model consists of one single block with a vertical recharge from a depth. The main objective of the study was to find out if the geothermal system was able to produce enough steam for 70 MWe generation for the life time of the project. The main conclusions were that production wells with feed zones at shallow depths (200 – 400 m b.s.l.) were not able to sustain

the 70 MWe generation. In order to maintain the 70 MWe, it was necessary to drill at least four new production wells in deeper zones (deeper than 400 m b.s.l.) at the northwestenr part of the field. It was also concluded that, the generating capacity of the system was not more than 35 MWe, with only shallow production wells and without reinjection of the brine.

In 1989, the second modeling study of Momotombo was conducted by DAL SpA. They used the same conceptual model of the previous one, but with a three dimensional numerical model that consists of 1051 grids covering 230 km^2 with a depth of 2100 m. Feature of the model is that a reservoir grid is coupled with a wellbore model: DPOZZO to simulate flow conditions at the surroundings of the wells in a reservoir grid, and POZZO to simulate the fluid flow from a single feed zone up to the wellhead. Objectives of this study were to confirm the production capacity enough for 70 MWe generation for 25 years. The results show a decline of the power output from the date of commissioning the second unit (March 1989) for a scenario without new wells and reinjecting 400 t/h of brine. Then, it was concluded that drilling new deep wells at the NW part of the field is needed to sustain the 70 MWe power output.

Reservoir simulations using and updated model with the same code were conducted in 1991 by using more field data: production data, downhole pressure and temperature profiles, and geological data. The main purpose of the simulation was to locate and depths of the new wells to be drilled.

The last model was developed in 1994 by improving the two previous models. The mesh system covered an area of 270 km^2 with a thickness of 3000 m, which was divided into 8 x 10 x 8 (layers) elements. The main objective of this study was to improve the previous model in order to find the most probable production capacity of the Momotombo geothermal system. For this purpose, new information on geology and rock properties for deep layers were given. Another objective was to determine the probable generation without drilling new production wells, but under different reinjection scenarios, or drilling 4 deep wells and maintaining 100 % reinjection of the separated fluid. In order to increase the total power output and to examine the delay of the cooling effect due to reinjection, it was recommended to drill deep production wells. Consequently, the study suggested that having a 100% reinjection of the separated water, and a generation of 7 MWe per well, the field was capable to generate 20 MWe that is more than the installed capacity at that time (DAL SpA, 1994).

Many changes occurred in the Momotombo geothermal reservoir after 1994. Firstly, the reservoir pressure dropped at a rate of 2 bars/year and, this induced an extensive boiling in the shallow reservoir. Consequently, quick intrusion of low temperature water into the reservoir occurred and then resulted in cooling of the shallow reservoir (Arnorsson 1996, 1997 and 1998). At the same time, calcite scaling was formed in several production wells, and temperature declined at shallow wells, MT-5, 12, 17, 20 and 22, down to 170 – 180°C. As a result, these wells failed to discharge because of reservoir pressure decline and temperature drop as well, resulting in a drastic generation decline down to 8 MWe in 1999.

In year 2000, scaling was removed by mechanical cleaning from wellbores and acid jobs were carried out for wells which might suffered from scaling in the formation near wellbore, as well as drilling new deep wells. All these efforts for generation recovery succeeded in increase of power out put more than 20 MWe. Additional power of 7 MWe was performed with an OEC (ORMAT Energy Converter) unit.

6. CONCEPTUAL RESERVOIR MODEL

Forty-seven wells drilled in Momotombo provide a large amount of data of subsurface pressure and temperature, flow rates and fluid enthalpy, lithology, thermal alteration and chemistry. For example, more than 1200 temperature measurements and 1100 pressure measurements in wells were conducted from 1974 up to 2003. These data serve basic and necessary information to define initial reservoir conditions as well as transients due to exploitation of the field.

Fig. 5 shows a temperature cross-section (refer to Fig. 1 for location) through the Momotombo reservoir. The represents the major features in the subsurface fluid flow before exploitation: 1) Upflow zone indicated by isothermal line of 275°C located near wells MT-36 and MT-11. 2) Low temperature intrusion presents in the east, near MT-30. 3). Most shallow production wells have their water loss zone in a temperature range from 225-250°C.

Fig. 6 shows the temperature distribution at 500 m b.s.l. which reveals similar conclusions as given by the cross section in Fig. 5. Two features in terms of temperature can be found in the field: 1) the so-called Bjornsson fault and 2) the shallow reservoir extending to the east. For space reasons we cannot present all the available initial temperature cross-sections, nevertheless we can comment that the Bjornsson fault is predominant as a hot structure from 600 m b.s.l. and deeper. Below 1300 m b.s.l., on the other hand, there appears to be a circular upflow zone with well MT-04 at the center, but this circular shape may change direction and become elliptical between WNW-ESE at these greater depths.

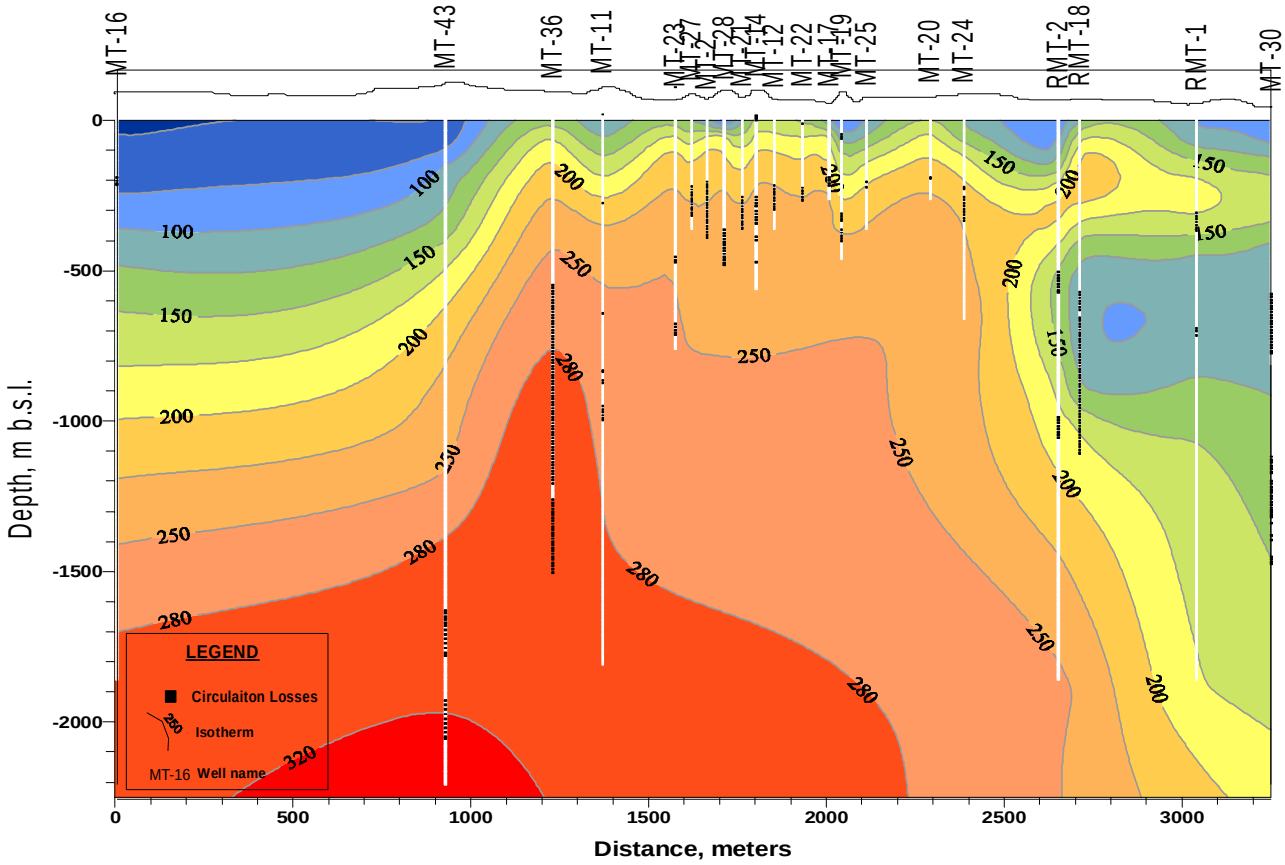

Figure 5: Selected temperature cross section across the center of the well field

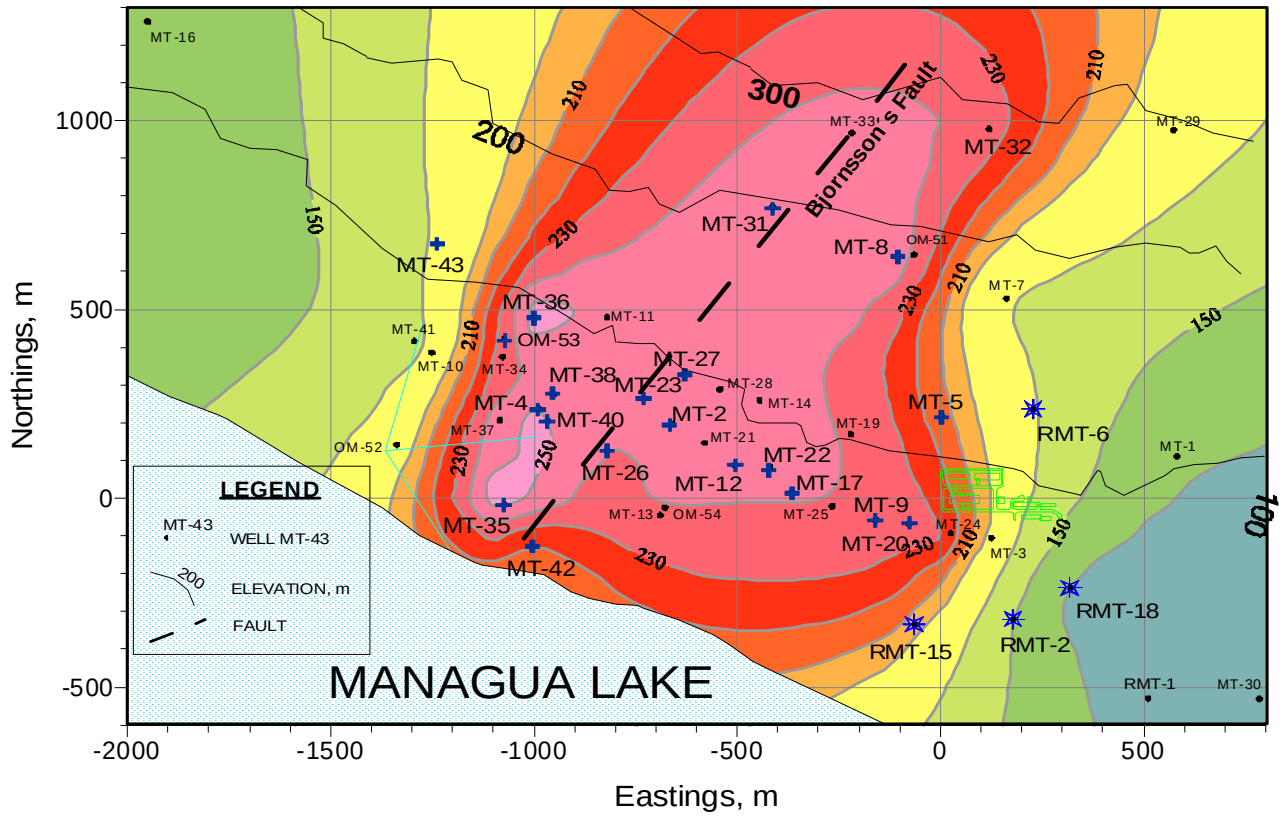

Figure 6: Temperature plain view at 500 m b.s.l.

7. NUMERICAL MODEL

Fig. 7 shows the plain view of grid system projected on a topographic map of the Momotombo area. Fig. 8represents the enlarged area where the exploitation area is located. A rectangular area of 13.8 km by 9.4 km was selected for grid system of numerical model with 3 km depth. The model consists of 207 grid blocks in a size range from 200 m x 200 m to 2 km x 2 km. In a vertical direction, the model was divided into nine layers with different thickness. The developed field for production and reinjection locates in the middle of the model with 2 km x 2.2 km, which consists of the blocks with 200 m x 200 m. Fig. 8 also shows the grid number and the grid center (by a green cross symbol (+)) with wells included into the mesh system (red cross for production wells, blue stars for reinjection wells and black cross for non-production wells). The mesh axes are oriented in parallel to the main faults which are intersected by most of the production wells, which, at the same time, are almost perpendicular to the Bjornsson fault (Fig. 6) intersected by the intermediate and deep production wells. This grid system obeys for a criterion based on location of the main faults that allows the circulation of fluid as well as to locate each active well in a different grid. There is an exception on three of them: one of these elements has two wells and the other two with three wells. The criteria of one well per grid will allow us to avoid any extreme pressure drop due to high production rate from one specific grid.

As for pre-processor for building grid system, Mulgeom was used. Mulgraph (O'Sullivan, 1995) was also used as post and pre-processors.

Fig. 9 shows the cross section of the model with layers and their thickness. The location of the main feed zones for all the wells in Momotombo is also plotted with different symbols. Non-production wells are those with water loss circulation during drilling, but they can't be used for production due to casing problems or drilling failure. Table 1 summarizes the depths of bottom and top of layer as well as the depth of centers and thickness of each of the nine layers in the model.

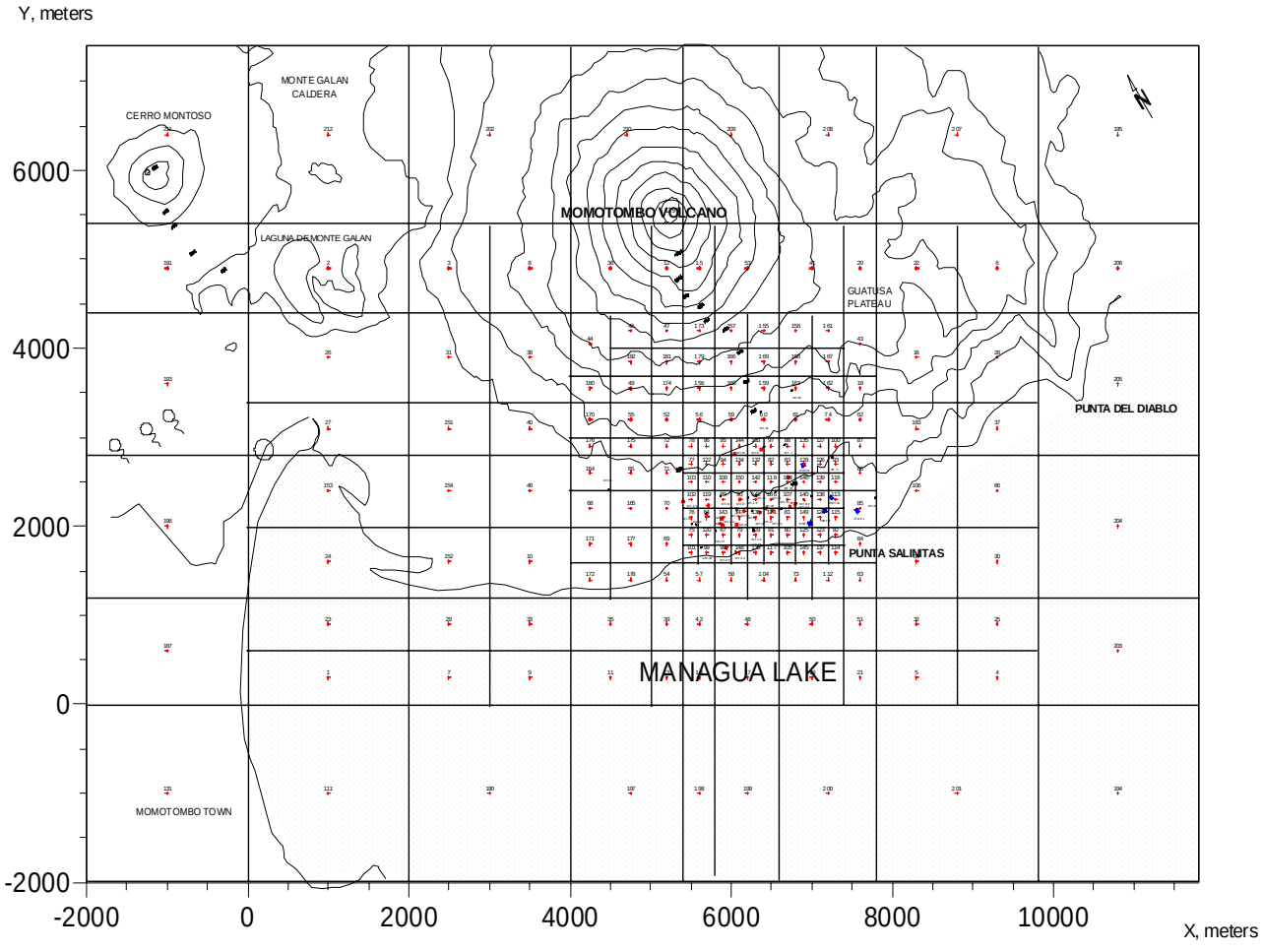

Figure 7: Mesh and topographic map of the Momotombo area

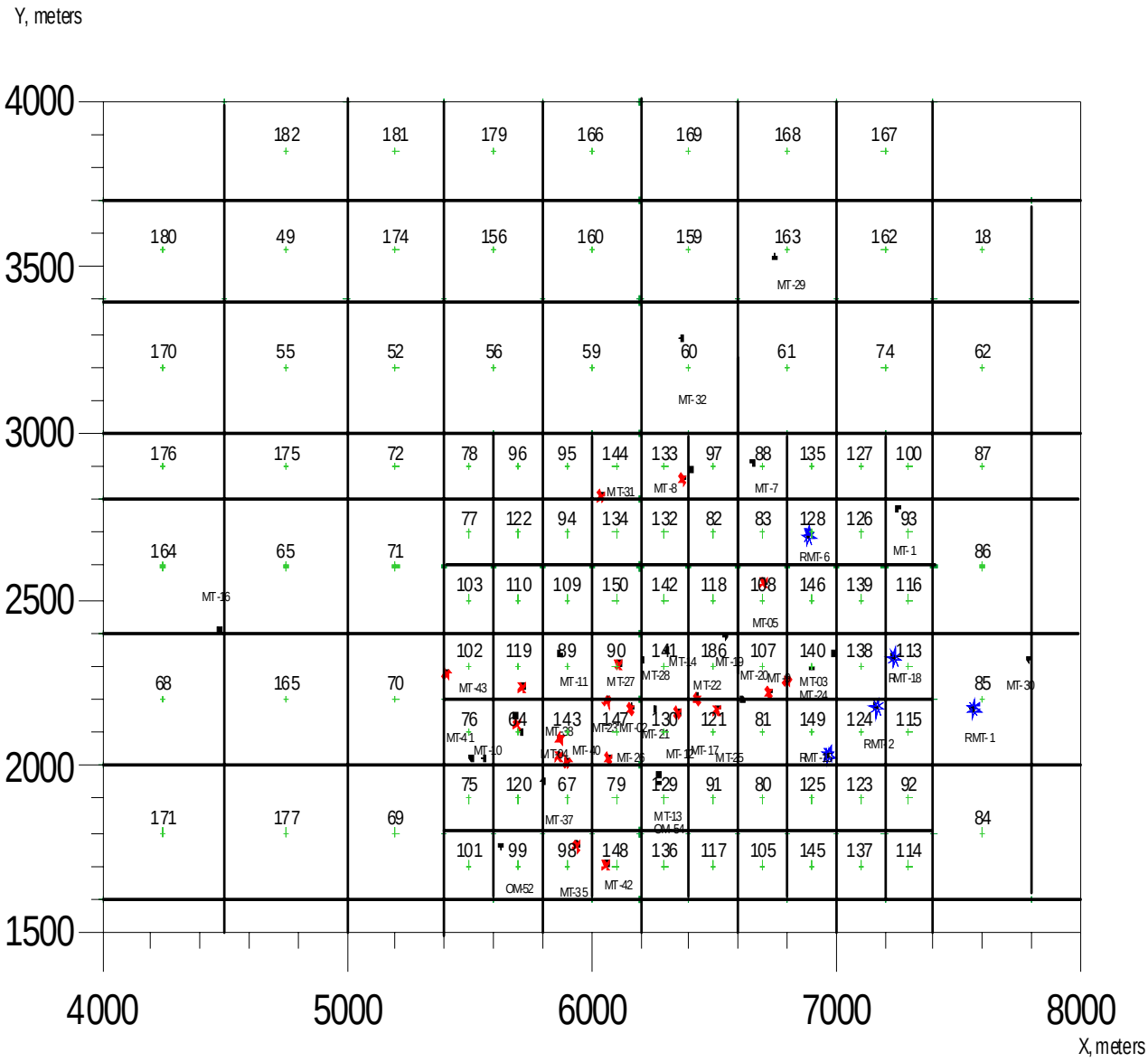

Figure 8: Zoom on the inner mesh where the exploitation area is located

There are three main permeable zones: a shallow one between 200 and 700 m b.s.l., another one is located between 700 and 1500 m b.s.l., and a deep zone is located between 1500 and 2000 m b.s.l.. Water loss zone of most of the wells are located in the shallow zone as shown in Fig. 9. This zone is thus divided into four layers for grid system, they are: BB, CC, DD and EE layers. These four layers were also necessary to represent the low temperature inflow to the system, which was identified by minerology and temperature distribution at the depth of 400 to 700 m b.s.l. in the eastern part of the field. This low temperature fluid moves below a lateral flow of high temperature. Another reason for thin layers is to express two-phase zone formed in the shallow zone.

On the other hand, layers FF, GG and HH represent the deeper permeable zones of the system where a liquid phase condition during production remains, and a relatively low number of production wells are located. This allowed us to assign thicker layers below 700 m b.s.l..

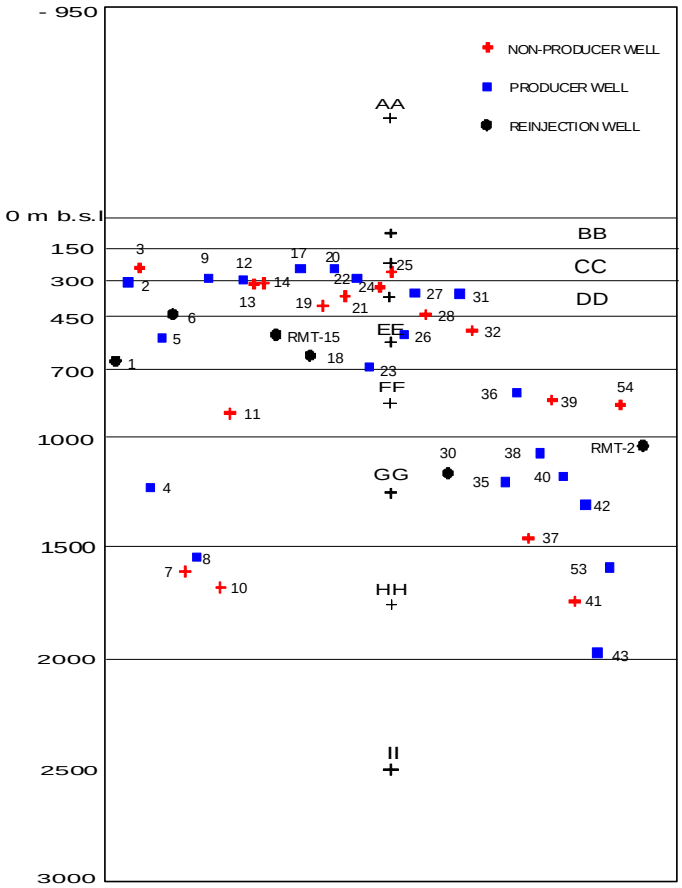

Figure 9: Layers of the model and location of main feed zones of Momotombo wells

Layer AA represents the surface blocks of the system. Its thickness is variable since our system is located at the slope of the Momotombo volcano, then surface elevation of blocks was given in a range from 950 m down to 40 m above sea level, then the thickness of layer AA ranges from 0 m and 950 m.

Layer II represents the bottom layer of the system. The depth of layer II is 3000 m b.s.l., which is determined from drilling and geological data.

An interference test carried out from November 2000 to August 2001 was analyzed by applying different reservoir models of porous type (Porras et. al, 2003). The best match between the observed and the calculated pressures was attained with a model in the presence of an impermeable boundary, and active wells located at the shallow reservoir (200 – 400 m b.s.l.). Estimated permeability-thickness product was 1.27 x 10^{-7} m^3/Pa.

Table 1: Depths and thickness of layers

Name of Layer	Depth m b.s.l.	Thickness m	Depth of grid center m b.s.l.
BB	0 to 150	150	75
CC	150 to 300	150	225
DD	300 to 450	150	375
EE	450 to 700	250	575
FF	700 to 1000	300	850
GG	1000 to 1500	500	1250
HH	1500 to 2000	500	1750
II	2000 to 3000	1000	2500

On the other hand, the rock properties assigned to the model considers permeability values between 10^{-17} and 5 x 10^{-13} m^2, given the maximum value to the permeable layer where shallow wells are located (150 – 450 m b.s.l.).

For the up flow zone, a relatively high permeability was initially assigned to the z direction. The porosities are given in a range from 0.06 and 0.20. Low porosity values are assigned to blocks with low permeability and the highest porosity value to blocks representing faults and very permeable zones (rock types CUPF, HIGH1 and HIGH2). For atmospheric blocks a porosity value of 0.25 was assigned. All other rock parameters are summarized in Table 2 for the best model for natural simulation.

Table 2: Rock properties for the best model

Rock type	Density (kg/m^3)	Porosity (-)	Permeability (m^2)			Thermal conductivity (W/m°C)	Spec. Heat capacity (J/kg°C)
			kx	ky	kz		
LOW	2500	0.08	8.33E-15	8.33E-15	1.75E-16	2.3	900
VLOW	2500	0.06	2.80E-16	2.80E-16	4.17E-16	3.0	900
MED3	2500	0.06	3.27E-13	3.27E-13	1.35E-14	2.3	900
MED2	2500	0.2	2.83E-15	2.83E-15	1.00E-16	2.3	900
UPFLO	2500	0.2	6.36E-15	6.36E-15	5.73E-14	2.3	900
MED1	2500	0.2	5.34E-13	5.34E-13	6.17E-13	2.3	900
HIGH2	2500	0.2	5.44E-13	5.44E-13	3.04E-12	2.3	900
ATM	2500	0.25	1.00E-13	1.00E-13	1.00E-13	5.5	1.0E+04
CUPF	2500	0.1	7.00E-14	7.00E-14	5.00E-16	2.5	1000
HIGH1	2500	0.2	5.44E-13	5.44E-13	3.04E-12	2.5	900
BOUND	2500	0.2	5.00E-15	5.00E-15	5.00E-15	2.3	1.0E+50
STEAD	2500	0.2	5.00E-15	5.00E-15	5.00E-15	2.3	900
CAPRK	2500	0.2	1.00E-20	1.00E-20	6.10E-16	4.3	900
CIRCL	2500	0.08	7.12E-14	7.12E-14	7.73E-17	2.3	900
DEEPR	2500	0.2	5.02E-16	5.02E-16	5.02E-16	2.3	900
EASTR	2500	0.2	1.69E-14	1.69E-14	1.69E-14	2.3	900

The rock type distribution is given in Fig. 10. Sixteen rock types were used for assigning different permeability values based on hydrogeological characteristics of the system and optimization of the rock type distribution. The VLOW rocktype was assigned to impermeable boundary located at the eastern part of the field that was defined by geophysical and geological studies, and it corresponds to the impermeable boundary reported by Porras, et.al (2003). For the cap rock of the geothermal system, the CAPRK rock type was assigned to layers AA and BB, having the lowest permeability values of the model (Table 2). Lateral boundaries were represented by assigning a specific rock type (BOUND) with the same permeability in all directions and high specific heat capacity to represent constant temperature. At the same time, for layer GG another rock type was assigned (STEAD) with the same rock properties as BOUND, with the only difference with the specific heat capacity being given 900 J/kg°C, and that these specific elements will be inactive by assigning a negative volume.

For blocks without geological information, the CIRCL rock type was assigned for layers GG up to CC, having a relatively low porosity (8 %) and low the permeability value on z direction. For layers HH and II, DEEPR rock type was assigned since geology suggests a low permeability at depth. For blocks surrounding the well field, the LOW rock type was assigned for all the layers except layers AA and BB. ATM represents the atmosphere that is represented by one big block filled with water at 15°C and 1 atm.

8. MODEL CALIBRATION

The simulated results for natural state were compared with temperature profiles of 31 wells and a vertical profile of reservoir pressure derived from measured pressure at main feed zones. This matching procedure was conducted mainly by adjusting permeability of rock types, flow rate and enthalpy of recharge assigned at the bottom grids. However, a further modification of the model is required to obtain better match. They consist of surface discharge and boundary conditions for lateral flow. These modifications need a lot of computing time and tedious work on input data. Thus, inversion technique for this job was adopted by using iTOUGH2 (Finsterle, 1999), which was run on the parallel computer at Orkustofnun, Iceland.

Parameters to be identified by iTOUGH2 are summarized in Table 3. There are 41 different kinds of parameters. As for natural state simulation, parameters except productivity index of wells are to be identified. Their values are set in a certain range in which iTOUGH2 automatically improve them during iterations to attain good fit between measured and simulated temperatures of wells. Then, estimated parameters above are given as initial conditions for a subsequent history matching simulation.

Table 3: Parameters to be identified by inversion using iTOUGH2

Parameter	Description	Parameter	Description	Parameter	Description
heat_loss	Heat loss at well field	por3-z	kz for MED3	PI_MT-22	P.I. Well MT-22
big-inf	Recharge flow rate	por4-z	kz for MED2	PI_MT-23	P.I. Well MT-23
enth	Recharge enthalpy	por5-z	kz for UPFLO	PI_MT-26	P.I. Well MT-26
por1-xy	kx, ky for LOW rock	por6-z	kz for MED1	PI_MT-27	P.I. Well MT-27
por2-xy	kx, ky for VLOW rock	circl-z	kz for CIRCL	PI_MT-31	P.I. Well MT-31
por3-xy	kx, ky for MED3 rock	por8-z	kz for HIGH1	PI_MT-35	P.I. Well MT-35
por4-xy	kx, ky for MED2 rock	cond_heat	Heat at bottom layer	PI_MT-36	P.I. Well MT-36
por5-xy	kx, ky for UPFLO rock	PI_hotspr	P.I. At surface disch	PI_MT-42	P.I. Well MT-42
por6-xy	kx, ky for MED1 rock	PI_MT-2	P.I. Well MT-2	PI_MT-43	P.I. Well MT-43
circl-xy	kx, ky for CIRCL rock	PI_MT-5	P.I. Well MT-5	PI_MT-53	P.I. Well MT-53
por8-xy	kx, ky for HIGH1 rock	PI_MT-8	P.I. Well MT-8	PI_MT-48	P.I. Well MT-4,38,40
CAPRK-z	kz for CAPRK rock	PI_MT-12	P.I. Well MT-12	DEEPR	kx, ky, kz for DEEPR
por1-z	kz for LOW rock	PI_MT-17	P.I. Well MT-17	EASTR	kx, ky, kz for EASTR
por2-z	kz for VLOW rock	PI_MT-20	P.I. Well MT-20	porosity	porosity for HIGH1, CUPF

P.I.: Productivity Index

During the course of history matching simulation, an objective function is defined as summation of residuals between measured and simulated values such as mass flow rates and enthalpies of twenty-one wells, and pressure draw down of four observation wells.

As residuals are available at each time of observation, they are put together and the results are analyzed for optimum values using non-linear least square method of Levenberg-Marquardt. Then, the estimated parameters in the history matching, except productivity indices of wells, are given as initial conditions for repeating a natural state simulation. Then, the same procedure is repeated for a history matching simulation and the value of objective function is compared with the previous one. This whole procedure is repeated until a discrepancy of the values of objective function satisfies a specified convergence criteria.

8.1 Temperature Profiles

Fig. 11 shows the comparison of measured and simulated temperature profiles of six wells obtained with the best model. They are MT-4, which is possibly located in the upflow zone at the western part of the field. MT-31 and 8 are located at the center of the well field, and MT-5 and RMT-6 are at the eastern part of the well field.

As shown in Figs. 11a,b,c,d,e most of the characteristics in temperature profiles are well reproduced with simulated results, such as near boiling point curve in well MT-04, low temperature water intrusion at MT-05, and a reverse profile in well RMT-6.

Fig. 11(f) shows matching between estimated initial pressures at main feed zone and simulated for selected wells. These wells were selected depending on feedzone depth and location as well as the quality of measured data. For data points of shallow wells MT-2 and 31, measured pressure seems to be higher than simulated ones. This may be because of lower measured temperature.

8.2 Location of Recharge Areas

The location of the recharge zone was determined as an initial guess on the basis of the analysis of the initial temperature distribution and geophysical data analysis. One hot recharge area was located at the western part of the well field. A lateral recharge with relatively low temperature exists at the eastern part of the well field; the origin of this recharge is not clearly defined, but it may be originated from Lake Managua, or intrusion of meteoric water. The model considers this recharge by assigning a constant pressure boundary with relatively low temperature at the eastern edge of the model. In order to match the temperature reversal (Fig. 11e), it was also necessary to place an impermeable boundary. This boundary was described by TRANSPACIFIC (2000) as a reservoir boundary and it was also pointed out by the mineralogical study (Down, 1992).

The result of an interference test analysis carried out by Porras (2003) suggested a presence of an impermeable boundary in the reservoir. The location of the boundary, however, cannot be specified from the results. The numerical model used for matching the pressure response of the reservoir confirmed its presence.

8.3 Flow rate and Enthalpy of Recharge

Flow rate and enthalpy of the recharge at the bottom was estimated to be 24.6 kg/s and 1700 kJ/kg. As for lateral recharge, pressure of the grid located outside of the system was kept constant and its value was estimated during natural state simulation.

8.4 Heat Flow

Heat flow was measured at two different places in Momotombo. An average heat flow was 0.083 W/m^2, obtained by measuring temperature at shallow wells. In order to create a thermal gradient in the model, this heat flow of 0.083 W/m^2 was firstly assigned to all the elements of the bottom layer II, but later it was defined as a parameter to be estimated by iTOUGH2, which resulted to be 3.7 times higher.

Surface discharges presented before fluid production in the field. Thigpen (1970) reported the existence of hot springs at Punta Salinitas as well as fumarole activities located close to the center of the well field and to the northeast near well MT-29 (Fig. 1). These surface discharges were considered in the model by assigning blocks on deliverability in order to express the discharge from the hot springs and fumaroles.

8.5 History Matching

History matching simulations were carried out for the period from 1983 to 2003. Fig. 12 shows the comparisons between the measured and the simulated results of total flow rate and enthalpy with time obtained for the best model. Four wells are selected for comparison, because of their relative good match. MT-12 is a shallow well representing shallow reservoir characteristics. This well produced dry steam for about four years, starting just after the second 35 MWe unit was commissioned in march 1989, but its high enthalpy can't be simulated. However, increment of enthalpy at $2x10^8$ seconds is observed both measured and simulated results. Marked discrepancies of enthalpy through out the period may be because of the differences of phase conditions in reservoir. On the other hand, flow rates show a relatively good match.

Well MT-23 shows a reasonably match in enthalpy except the later period when the measured values decrease with time. Flow rate only match in the latter period.

Good match in enthalpy is also observed for well MT-26, except for the latter period. Both measured and simulated flow rates present decreasing with time. Quick drop at $4.5x10^8$ seconds is because of scaling in the wellbore. A match in the latter period was satisfactory.

Fig. 13 shows comparison of pressure draw down for four wells, two wells, MT-11 and MT-13, show a relatively good match except in the latter part when measured pressure draw down remains constant whereas simulated ones markedly dropped.

Well MT-41 also shows a good match. However, match of well MT-30 was poor such that simulated values are below the measured ones throughout the period. This may be because of the high permeability of the grids that represent impermeable boundary located between the production zone and this well.

9. CONCLUSIONS

Main conclusions of this study are as follows:

1) A three-dimensional well-by-well numerical model of Momotombo geothermal reservoir has been developed.

2) Simulation using iTOUGH2 was conducted for natural state and history matching for the Momotombo geothermal field, Nicaragua.

3) Temperature profiles of wells for natural state simulation were well matched for most of them.

4) For history matching, relatively good match was obtained in flowrates and enthalpy for wells MT-23 and 26, but the match was poor for the enthalpy of the well producing dry steam (MT-12).

ACKNOWLEDGMENT

We thank ORMAT Momotombo Power Company for permission to publish their data and support. Also, special thanks to Mr. Grimur Bjornsson for revising and calibrating the model by using iTOUGH2.

REFERENCES

Arnórsson, S., Sánchez M., Miranda K.: Interpretation of geochemical and isotopic data from well discharges in the Momotombo Geothermal Field, Nicaragua with recommendations on monitoring studies. *Report* to IAEA, 41pp. (1996).

Arnórsson, S., Sánchez M., Miranda K.: Interpretation of geochemical and isotopic data on fluid discharge from well in the Momotombo Geothermal Field, Nicaragua. *Report* to IAEA, 68 pp. (1997).

Arnórsson, S., Sánchez M., Miranda K.: Interpretation of geochemical and isotopic data from well discharges in the Momotombo Geothermal Field, Nicaragua with notes on gas-chromatography analysis. *Report* to IAEA (1998).

Bjornsson G.S., Porras E.: Estimated temperature distribution in the Momotombo goethermal reservoir, based on 25 years of well logging. *Report* prepared for Ormat Momotombo Power Company, 68 pp. (2001).

DAL SpA: Campo Geotérmico de Momotombo: Optimización del sistema Campo-Planta. Informe final. *Internal report* INE (Instituto Nicaragüense de Energía), Managua, Nicaragua. DAL SpA, Milano, Italia (1989).

DAL SpA: Campo Geotérmico de Momotombo: Estudio de Factibilidad de la Tercera Unidad. Actualización del recurso. *Internal report* INE (Instituto Nicaragüense de Energía), Managua, Nicaragua. DAL SpA, Milano, Italia (1991).

DAL SpA: Campo Geotérmico de Momotombo: Modelado del campo. *Internal report* INE (Instituto Nicaragüense de Energía), Managua, Nicaragua. DAL SpA, Milano, Italia (1994)..

DAL SpA: Estudios de evaluación del potencial energético: Factibilidad de la estabilización y de la tercera unidad geotermoeléctrica del campo geotérmico de Momotombo, Fase IA: Investigaciones científicas; Informe de síntesis. *Internal report* ENEL (Empresa Nicaragüense de Electricidad), Managua, Nicaragua. DAL SpA, Milano, Italia (1995).

Down, M.: Minerología de alteración hidrotermal: Su aplicación en el estudio de la evolución del campo geotérmico de Momotombo. *Internal report* INE (Instituto Nicaraguense de Energía), 33 pp. (1995).

Electroconsult (ELC): Estudio de Factibilidad. Segunda Unidad de la Planta Geotérmica de Momotombo. *Internal report*. Reporte a INE (1983).

Finsterle, S.: iTOUGH2 Users Guide. *Report* LBNL-40040, Lawrence Berkeley National Laboratory, Berkeley, California (1999).

Geothermex: Plan Maestro Geotérmico de Nicaragua, Evaluación del área de Momotombo. *Internal report* Comisión Nacional de Energía de Nicaragua,Managua, Nicaragua. Geothermex, Inc., Richmond, California, USA, 97 pp. (2001).

O'Sullivan, M.J., and Bullivant, D.P.: A graphical interface for the TOUGH family of flow simulators. *Proceedings* of the TOUGH Workshop 1995, Berkeley,California, 90-95 pp. (1995).

Thigpen, J.B.: Final report: Geothermal Resources Project-Stage 1, Vols. 1, 7 and 10, Texas Instruments, Inc., *Internal* report to ENALUF (Empresa Nacional de Luz y Fuerza) (1970).

Trans-Pacific Geothermal Corporation.: Geophysical exploration of the Momotombo geothermal field,

Nicaragua. *Internal report*, ORMAT Momotombo Power Company. Trans-Pacific Geothermal Corporation, Oakland, California, USA 54pp. (2000).

Verma, M. P, E. Martínez., M. Sánchez, K. Miranda, J. Y. Gerardo and L. Araguas.: Hydrothermal Model of the Momotombo Geothermal System, Nicaragua. *Proceedings*, Twenty-First Workshop on Geothermal Reservoir Engineering, Stanford, Calif., January 22-24, 1996.

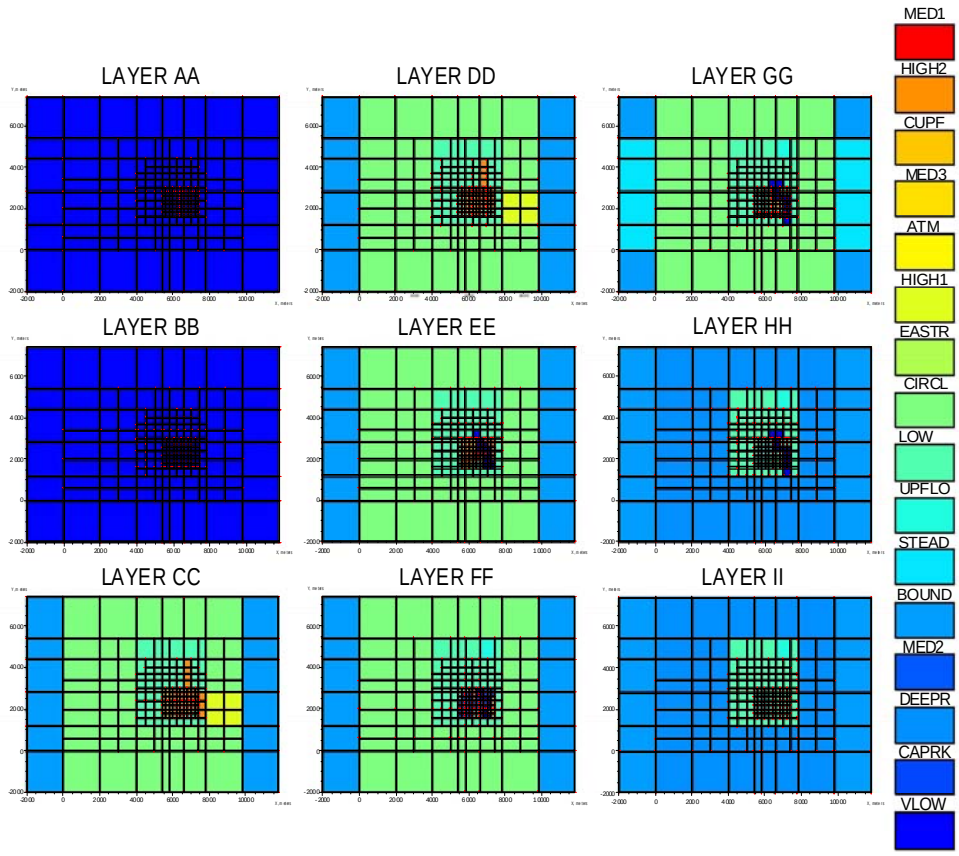

Figure 10: Rock type distribution of the numerical model

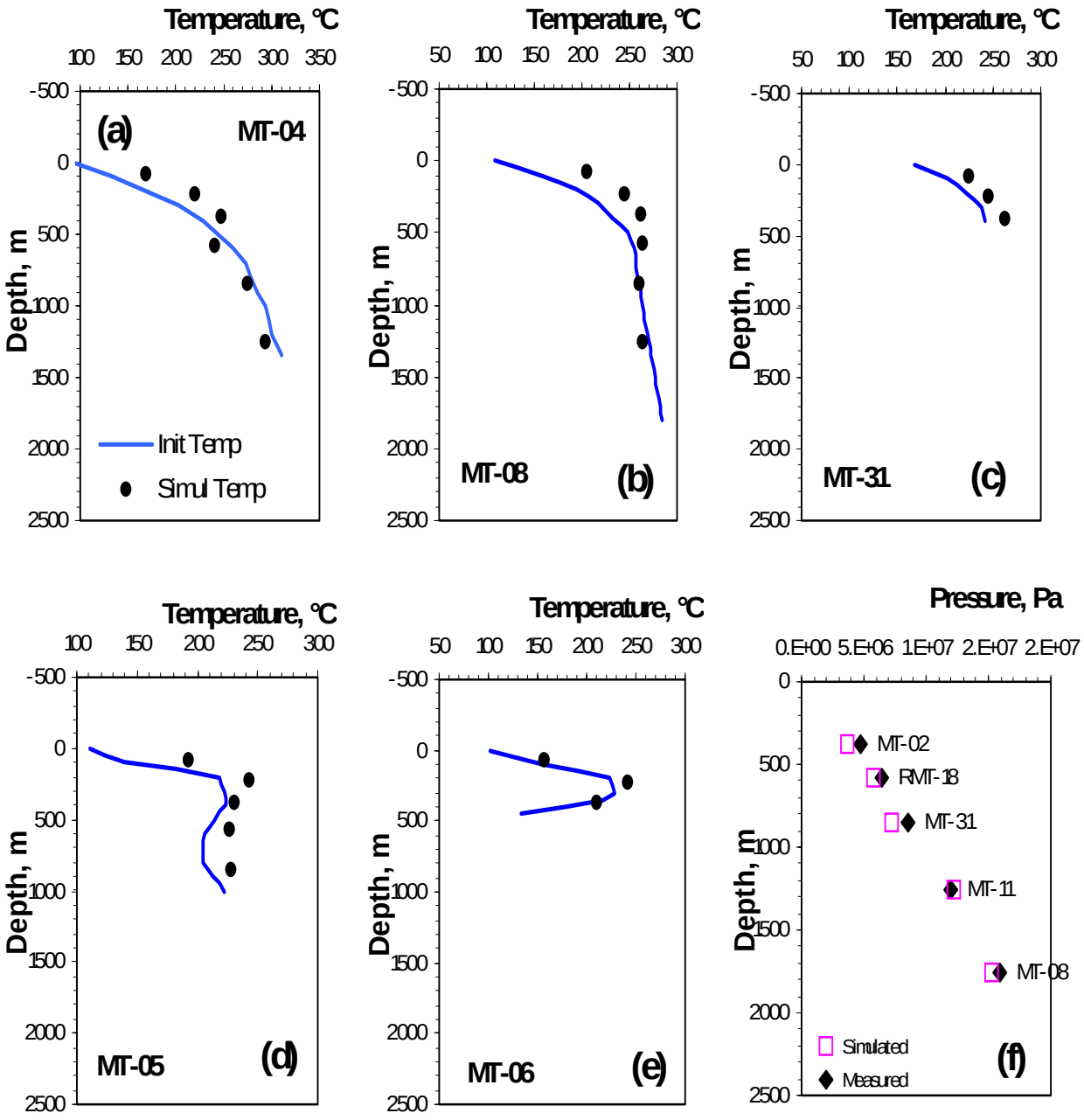

Figure 11: Initial and simulated temperature profiles, and pressure at main feed zones of five wells

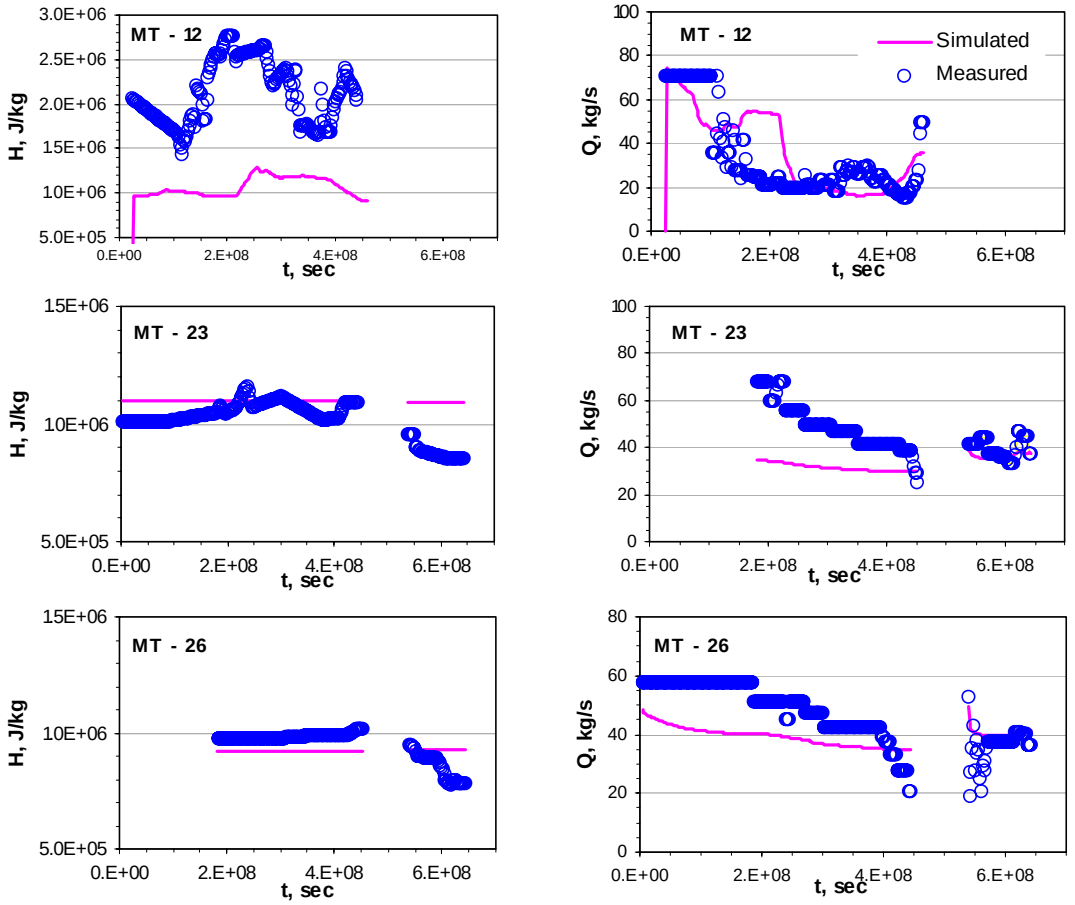

Figure 12: Total flowrates and total enthalpy calibration for selected production wells

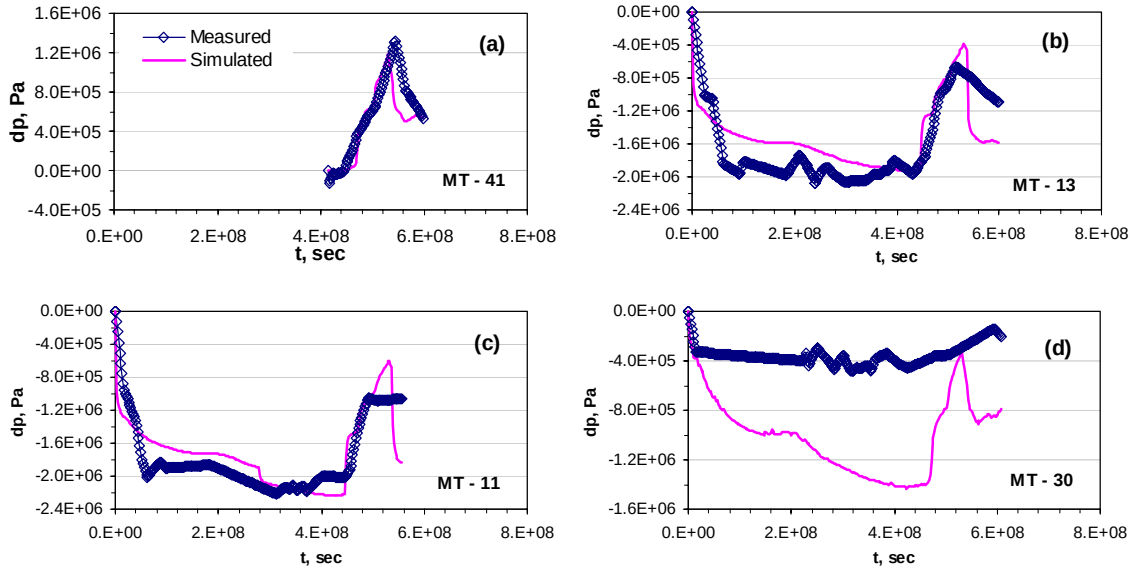

Figure 13: Pressure draw down calibration for four monitoring wells.